Available online at www.sciencedirect.com
SCIENCE DIRECT®
European Journal of Medicinal Chemistry 40 (2005) 467–472
EUROPEAN JOURNAL OF MEDICINAL CHEMISTRY
www.elsevier.com/locate/ejmech

Structural studies and cytotoxic activity of N(4)-phenyl-2-benzoylpyridine thiosemicarbazone Sn(IV) complexes

Anayive Perez-Rebolledo [a], José Danilo Ayala [a], Geraldo M. de Lima [a], Nicoletta Marchini [b], Gabriella Bombieri [b], Carlos L. Zani [c], Elaine M. Souza-Fagundes [c], Heloisa Beraldo [a,*]

[a] *Departamento de Química, Universidade Federal de Minas Gerais, 31270-901 Belo Horizonte, MG, Brazil*
[b] *Istituto di Chimica Farmaceutica e Tossicologica, Università di Milano, Viale Abruzzi 42, 20131 Milano, Italy*
[c] *Centro de Pesquisas René Rachou-FIOCRUZ, 30190-002 Belo Horizonte, MG, Brazil*

Received 21 October 2004; accepted 24 January 2005

Available online 24 February 2005

Abstract

Structural studies and an investigation of the cytotoxic activity of Sn(IV) complexes with N(4)-phenyl-2-benzoylpyridine thiosemicarbazone (H2Bz4Ph) were carried out. The crystal and molecular structures of $[Sn(2Bz4Ph)Cl_3]\cdot CH_3CH_2OH$ (**1**) and $[Sn(2Bz4Ph)BuCl_2]\cdot H_2O$ (Bu = butyl group) (**2**) were determined. Both compounds present octahedral coordination geometry with the 2Bz4Ph anionic ligand behaving as tridentate on the metal ion. A comparative study of the structures of these compounds along with that of $[Sn(2Bz4Ph)Bu_2Cl]$ (**3**) determined before is presented. The cytotoxicity of H2Bz4Ph and its Sn(IV) complexes was investigated against the MCF-7, TK-10 and UACC-62 human tumor cell lines. Among the three complexes, **3** proved to be better as cytotoxic agent than the clinically used drug etoposide. H2Bz4Ph and all complexes were able to induce apoptosis in UACC-62 cells.

Keywords: Thiosemicarbazones; Tin(IV) complexes; Crystal structures; Cytotoxic activity

1. Introduction

Thiosemicarbazones and their metal complexes present a wide range of bioactivities, and their chemistry and pharmacological applications have been investigated [1,2]. Thiosemicarbazones derived from 2-formyl and 2-acetylpyridine have been extensively studied by other authors [3–6] and by some of us [7–11]. A few complexes of 2-benzoylpyridine thiosemicarbazones were studied [12–16]. The literature reports that some N(4′)-dialkyl 2-benzoylpyridine thiosemicarbazones and their copper(II) complexes are active against human pathogenic fungi [12]. In a previous work we prepared 2-benzoylpyridine-derived thiosemicarbazones and a series of their 3d metal complexes. The ligand presented in vitro antifungal activity against *Candida albicans*, but this activity decreases or is lost on coordination [17].

Tin complexes are known for their interesting multiple applications as antitumorals, antibacterials, antifungals and biocides [18–20]. Coordination of tin with thiosemicarbazones could in principle give complexes with the therapeutic properties of both metal and ligands.

Recently some of us reported the spectral characterization and an investigation of the antifungal activity of N(4)-phenyl-2-benzoylpyridine thiosemicarbazone (H2Bz4Ph) and its tin(IV) complexes $[Sn(2Bz4Ph)Cl_3]\cdot CH_3CH_2OH$ (**1**), $[Sn(2Bz4Ph)BuCl_2]\cdot H_2O$ (**2**) and $[Sn(2Bz4Ph)Bu_2Cl]$ (**3**) (2Bz4Ph is the anionic ligand, formed upon deprotonation at N(3) and Bu = butyl group) [21]. Among the three complexes, **1** proved to be the most active as antifungal against *C. albicans*.

In the present work we report a structural study of complexes **1** and **2** as well as an investigation of the cytotoxicity of H2Bz4Ph and of complexes **1**–**3** against the MCF-7, TK-10 and UACC-62 human tumor cell lines.

2. Results and discussion

2.1. Crystal and molecular structures

Table 1 lists crystal data and structure refinement for complexes **1** and **2**. Tables 2 and 3 list selected bond lengths and

* Corresponding author.
E-mail address: hberaldo@ufmg.br (H. Beraldo).

0223-5234/$ - see front matter © 2005 Elsevier SAS. All rights reserved.
doi:10.1016/j.ejmech.2005.01.006

Table 1
Crystal data and structure refinement for complexes $[Sn(2Bz4Ph)Cl_3]\cdot CH_3CH_2OH$ (**1**) and $[Sn(2Bz4Ph)BuCl_2]\cdot H_2O$ (**2**)

Compound	(**1**)	(**2**)
Empirical formula	$C_{21}H_{21}N_4SOSnCl_3$	$C_{23}H_{26}N_4SOSnCl_2$
Formula weight	602.53	596.17
Color; habit	Yellow, prism	Yellow, prism
Crystal size (mm)	0.12 × 0.10 × 0.15	0.09 × 0.08 × 0.12
Crystal system	Monoclinic	Monoclinic
Space group	$P2_1/c$	$P2_1/n$
a (Å)	9.434(5)	8.848(5)
b (Å)	12.470(9)	14.225(9)
c (Å)	20.482(9)	20.487(9)
β (°)	91.98(7)	99.64(5)
Volume (Å^3)	2408(2)	2542(2)
Z	4	4
Density calc (g cm^{-3})	1.665	1.560
Temperature (K)	298	298
θ max (°)	25	20
Reflections measured	4229	3060
Observed [$I \geq 2\sigma(I)$]	2682	2185
Number of variables	324	277
h range	–11 to 11	–8 to 8
k range	–1 to 14	–1 to 13
l range	–1 to 24	–1 to 19
Empirical absorption	Psi scan	Psi scan
Scan method	Omega scan	Omega scan
Absorption coefficient (mm^{-1})	1.502	1.320
$F(000)$	1200	1200
R (obs./all)	0.045/0.10	0.041/0.046
wR_2 (obs./all)	0.14/0.16	0.10/0.11
Goodness-of-fit	1.1	1.2

Table 2
Selected bond distances (Å) for complexes $[Sn(2Bz4Ph)Cl_3]\cdot CH_3CH_2OH$ (**1**), $[Sn(2Bz4Ph)BuCl_2]\cdot H_2O$ (**2**), $[Sn(2Bz4Ph)Bu_2Cl]$ (**3**)* and H2Bz4Ph*

Bond	(**1**)	(**2**)	(**3**)	H2Bz4Ph
Sn–N2	2.191(7)	2.198(5)	2.338(19)	
Sn–S	2.430(3)	2.479(2)	2.507(10)	
Sn–N1	2.198(7)	2.268(5)	2.581(2)	
Sn–Cl	2.343(3)		2.613(2)	
Sn–Cl1	2.466(3)	2.529(2)	–	
Sn–Cl2	2.407(3)	2.491(2)	–	
Sn–C21		2.132(7)	2.159(9)	
Sn–C25			2.152(9)	
S–C8	1.756(8)	1.737(7)	1.736(3)	1.663(2)
N1–C2	1.351(11)	1.341(8)	1.345(3)	1.343(2)
N1–C6	1.314(11)	1.323(8)	1.328(4)	1.335(3)
N2–N3	1.345(9)	1.364(7)	1.378(3)	1.362(2)
N2–C7	1.299(10)	1.290(8)	1.305(3)	1.296(2)
N3–C8	1.313(10)	1.313(8)	1.314(3)	1.360(2)
N4–C15	1.393(11)	1.411(9)	1.426(3)	1.410(2)
N4–C8	1.356(10)	1.349(8)	1.358(3)	1.343(3)

* Ref. [17].

angles for complexes **1** and **2**, respectively, as well as those for complex **3** [21] and H2Bz4Ph for comparison. Table 4 shows a comparison of the bond lengths in the Sn coordination spheres of related compounds.

Table 3
Selected bond angles (°) for complexes $[Sn(2Bz4Ph)Cl_3]\cdot CH_3CH_2OH$ (**1**), $[Sn(2Bz4Ph)BuCl_2]\cdot H_2O$ (**2**), $[Sn(2Bz4Ph)Bu_2Cl]$ (**3**)* and H2Bz4Ph*

Angle	(**1**)	(**2**)	(**3**)	H2Bz4Ph
Cl–Sn–Cl1	89.79(10)			
Cl–Sn–Cl2	91.98(10)			
Cl1–Sn–Cl2	171.25(8)	166.26(6)		
C21–Sn–C25			153.10(14)	
N1–Sn–Cl	99.01(19)		131.71(5)	
N1–Sn–S	154.8(2)	151.0(1)	142.02(5)	
N2–Sn–N1	74.3(2)	72.4(2)	66.19(7)	
N2–Sn–S	80.6(2)	78.8(2)	75.98(5)	
N2–Sn–Cl	172.5(2)		162.07(5)	
N3–N2–C7	120.0(7)	119.0(5)	114.59(19)	119.4(2)
C8–N3–N2	115.2(7)	115.7(5)	115.48(19)	120.5(2)
N4–C8–N3	119.1(7)	118.3(6)	116.8(2)	114.3(2)
N4–C8–S	112.0(6)	113.7(5)	114.96(19)	128.0(1)

* Ref. [17].

The trichloro complex **1** is in the *mer* configuration with the ligand acting as tridentate determining a distorted octahedral coordination geometry (Fig. 1). The hexa-coordinated tin is bonded to three chlorines, two nitrogens and one sulfur. In the meridional configuration of the three chlorines, two *trans* to each other, the bond distances are rather asymmetric but on average significantly larger than that of the chlorine *trans* to the nitrogen. When H2Bz4Ph is coordinated to tin in $[Sn(2Bz4Ph)Cl_3]\cdot CH_3CH_2OH$ (**1**) $[Sn(2Bz4Ph)BuCl_2]\cdot H_2O$ (**2**) and $[Sn(2Bz4Ph)Bu_2Cl]$ (**3**) [21] (reported for comparison), the metal-to-ligand bond distances progressively increase from complex **1** to complexes **2** and **3**, due to the spatial requirements of the rather bulky butyl groups that force the ligand to back off from the tin atom.

The molecular packing of **1** shows an interesting interaction between adjacent molecules involving N4–H41 and Cl1 (N4–H41...Cl1″ 2.50(8) Å, 175(8)° and N4...Cl1″ 3.350(8) Å (″ at $-x$, 0.5 + y, 0.5 – z) with the formation of molecular chains as shown in Fig. 2. This relatively short contact could be responsible of the lengthening of the Sn–Cl1 bond distance (2.466(3) Å) with respect to the *trans* Sn–Cl2 (2.407(3) Å). In the H2Bz4Ph free ligand [21] the molecular cohesion was determined by π interactions between the conjugated sys-

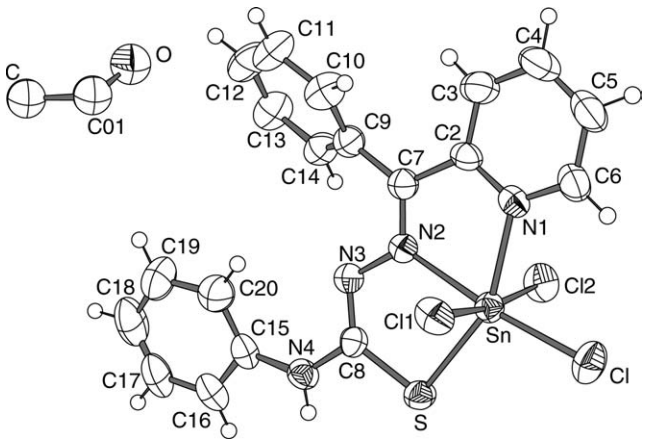

Fig. 1. ORTEP view of $[Sn(2Bz4Ph)Cl_3]\cdot CH_3CH_2OH$ (**1**) (ellipsoids are at 50% probability).

Table 4
Comparison of the bond lengths (Å) in the Sn coordination spheres of related compounds

Compound	Sn–Cl_{ap}	Sn–Cl_{eq}	Sn–N_{py}	Sn–N	Sn–C	Sn–S	References
[Sn(2Bz4Ph)Cl_3]·CH_3CH_2OH	2.466(3) 2.407(3)	2.343(3)	2.198(7)	2.191(7)		2.430(3)	
[Sn(2Bz4Ph)$BuCl_2$]·H_2O	2.529(2) 2.491(2)		2.268(5)	2.198(5)	2.132(8)	2.479(2)	
[Sn(2FPT)Cl_3]	2.433(1) 2.415(1)	2.360(1)	2.225(3)	2.194(2)		2.463(1)	[24]
[Sn(2Bz4Ph)Bu_2Cl]		2.613(2)	2.581(7)	2.338(7)	2.159(9)	2.507(1)	[17]
[Sn(Hapt)$BuCl_2$](1.5H_2O)	2.551(4) 2.486(4)		2.29(1)	2.20(1)	2.13(1)	2.493(4)	[25]
[Sn(Hapt)$PhCl_2$](C_2H_5OH·H_2O)	2.507(1) 2.476(3)		2.237(7)	2.226(7)	2.150(8)	2.481(2)	[25]

2Bz4Ph: N(4)-phenyl-2-benzoylpyridine thiosemicarbazonato. FPT: 2-formylpyridine thiosemicarbazone. Hapt: 2-acetylpyridine thiosemicarbazone.

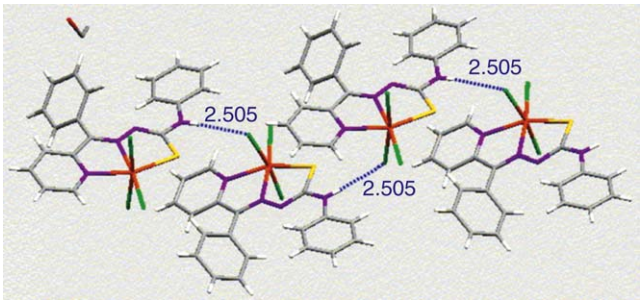

Fig. 2. Intermolecular H bond interaction in compound [Sn(2Bz4Ph)Cl_3]·CH_3CH_2OH (**1**).

tems of the thiosemicarbazone moieties of the molecules centrosymmetrically related as depicted in Fig. 3 with two relatively short contacts N4...N4′ 3.554(6) and N3...N4′ 3.717(6) Å between molecules related by inversion center.

The dichloro complex **2** having a butyl group instead of one chlorine has the same Sn coordination geometry of **1** (Fig. 4). The presence of the bulky ligand causes a lengthening of both the axial Sn–Cl bond distances due to the steric hindrance of the butyl group. Water molecules, detected in the crystal cell, connect adjacent complex units by H bond interactions with chlorines of two different molecules as H bond donor and as acceptor of an H coming from N4–H of a third molecule in a tridimensional net work as shown in Fig. 5 (for sake of clarity only three molecules are reported). Significant contacts are represented by O1–H1...Cl1 2.361(2) Å

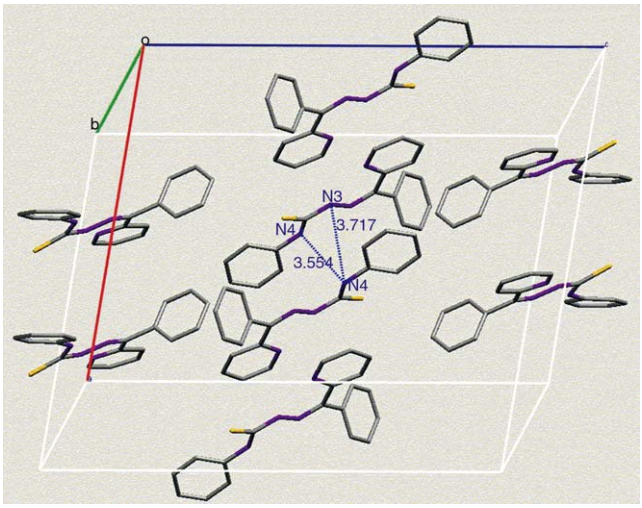

Fig. 3. Molecular Packing of H2Bz4Ph (the shorter distance is between N4...N4′ (at 1 – *x*, 1 – *y*, 1 – *z*).

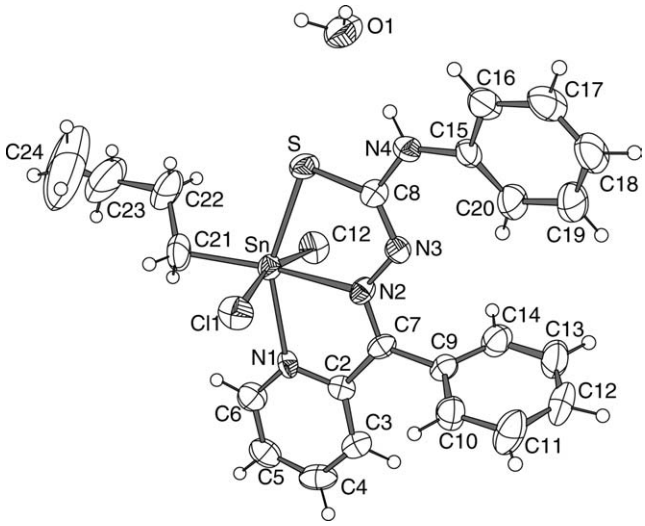

Fig. 4. ORTEP view of [Sn(2Bz4Ph)$BuCl_2$]·H_2O (**2**) (ellipsoids are at 40% probability).

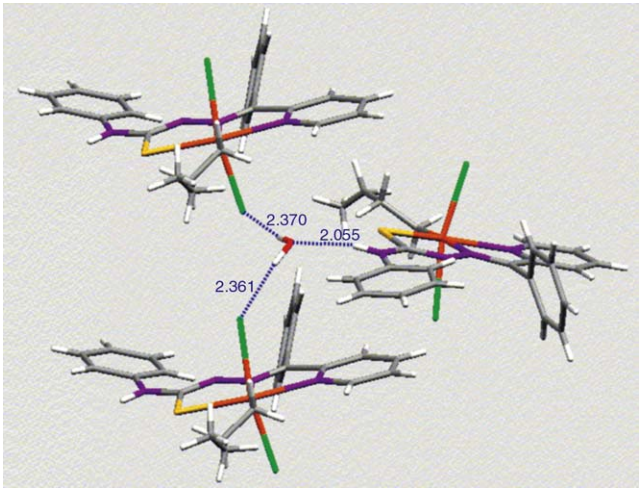

Fig. 5. Intermolecular H bond interactions in compound [Sn(2Bz4Ph)$BuCl_2$]·H_2O (**2**).

172(7)°, O1–H2...Cl2 2.370(2) Å, 169(7)° and O1...H–N4 2.055(6) Å, 168(1)° (1.5 – *x*, 0.5 + *y*, 0.5 – *z*, 0.5 – *x*, 0.5 + *y*, 0.5 – *z*).

Upon complexation the C8–N3 bond length changes from 1.360(2) Å in H2Bz4Ph to 1.313(10) Å in complex **1**, 1.313(8) Å in **2** and 1.314(3) Å in **3** and the C8–S bond distance varies from 1.663(2) Å in H2Bz4Ph to 1.756(8) Å in complex **1**, 1.737(7) in **2** and 1.736(3) Å in complex **3**, consequent to the N3 deprotonation with the formation of an extensively con-

jugated system involving the thiosemicarbazone moiety and the two rings attached to C7. The C–S bond length goes from thione in the free ligand to thiolate in the complexes and C8–N3 from a single bond in H2Bz4Ph to a predominantly double bond in the complexes. The N2–N3 and N2–C7 bond distances do not change significantly upon coordination (Table 2).

In [Sn(FPT)Cl_3] [22], the C–S bond distance, 1.753(3) Å, is essentially the same as in complex **1** and comparable to that of complexes **2** (1.737(7) Å), and **3** (1.736(3) Å). All are in agreement with deprotonation upon complexation and formation of a C–S single bond. All metal-to-ligand bond distances are larger in complex **1** than in the 2-formylpyridine analogue [23], as a consequence of the bulk H2Bz4Ph ligand, not allowing a closer interaction with the Sn center. The angles within the thiosemicarbazone moiety undergo significant modifications on coordination, with a shrinking of the C8–N3–N2 angle from 120.5(2)° in the ligand to 115.2(7)° in complex **1**, 115.7(5)° in **2** and 115.5(2)° in **3**; and of the N4–C8–N3 angle from 114.3(1)° in the ligand to 119.1(7)° in complex **1**, 118.3(6)° in **2** and 116.8(2)° in **3**, in order to match the steric requirements for tridentate coordination (Table 3).

All the angles around the metal center decrease in going from complex **1** to complexes **2** and **3** due to the presence of one and two bulky butyl groups in **2** and **3**.

Significant differences were found in the angles between the plane of the thiosemicarbazone moiety and that of the pyridine ring, being 10.86(3)° in H2Bz4Ph [21], 7.9(2)° in **1**, 3.1(2)° in **2** and 8.6 (2)° in **3** [21]. The angles between the thiosemicarbazone chain and the N(4)-phenyl ring are also different: 26.0(3)° in H2Bz4Ph, 16.7.(3)° in **1**, 18.6(6)° in **2** and 37.6 (3)° in **3**.

It is interesting to observe the variations in the bond distances in the coordination sphere according to the number of the coordinated chlorines, that influence the Lewis acidity of the tin cation, which is higher in the trichloro complex. The consequence is a strong covalency for the metal–nitrogen bond but in a minor extent also for the metal–sulfur bond, as shown in Table 4, where the bond distances in the Sn coordination sphere are compared for **1**, **2** and related complexes.

The packing forces play also an important role in the bond distances, particularly in the presence of intermolecular contacts as in the examined compounds. The different Sn–Cl bond lengths could be explained by the presence of Cl...H intermolecular interactions as described before. In fact, also for compound **3** [21], besides the lengthening of the bond distances in the coordination sphere attributed to the bulkiness of the coordinated butyl groups, the large equatorial Sn–Cl bond length of 2.613(2) Å could be ascribed to the intermolecular contact Cl...H41 of 2.54(1) Å with adjacent molecules, determining the polymeric chain shown in Fig. 6.

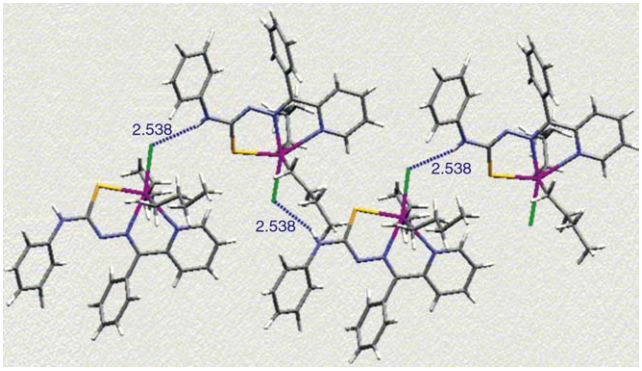

Fig. 6. Intermolecular H bond interactions in compound [Sn(2Bz4Ph)Bu_2Cl] (**3**).

2.2. Cytotoxic activity

Table 5 lists the compound concentration that produces 50% of growth inhibition (IC_{50}) and the compound concentration that kills 50% of cells (LD_{50}) for H2Bz4Ph and its tin(IV) complexes against the MCF-7, TK-10 and UACC-62 human tumor cell lines, along with the corresponding values of IC_{50} and LD_{50} for the clinically used drug etoposide for comparison.

The IC_{50} and LD_{50} values are lower for H2Bz4Ph and all its tin(IV) complexes than for etoposide against the MCF-7 and TK-10 cell lines. Moreover, IC_{50} and LD_{50} of H2Bz4Ph and complex **3** are lower than that of etoposide against the UACC-62 cell line. Of all compounds, complex **3** showed the better results, with values of IC_{50} and LD_{50} 10–100 times lower than etoposide against the three cell lines.

2.3. Effect of N(4)-phenyl-2-benzoylpyridine thiosemicarbazone (H2Bz4Ph) and its tin complexes (*1–3*) on viability and apoptosis induction in UACC-62 cells

Considering that many cancer chemotherapeutic agents exert their cytotoxic activity by indirectly inducing apoptosis

Table 5
Compound concentration producing 50% of growth inhibition (IC_{50}) and killing 50% of cells (LD_{50})

Compound		Results (μM)					
		MCF-7		TK-10		UACC-62	
		IC-50	LD-50	IC-50	LD-50	IC-50	LD-50
	Etoposide	0.029	97.4	20.4	>169.9	3.1	>169.9
	H2Bz4Ph	<0.003	13.3	9.3	12.9	<0.003	13.8
(**1**)	[Sn(2Bz4Ph)Cl_3]	<0.002	24.2	16.4	23.1	9.7	>431.3
(**2**)	[Sn(2Bz4Ph)$BuCl_2$]	<0.002	24.2	17.3	21.8	1.2	>173.0
(**3**)	[Sn(2Bz4Ph)Bu_2Cl]	0.003	1.5	2.3	11.5	0.5	9.3

IC-50 = grow inhibition for 50% to the cells; LD-50 = lethal dose for 50% to the cells.

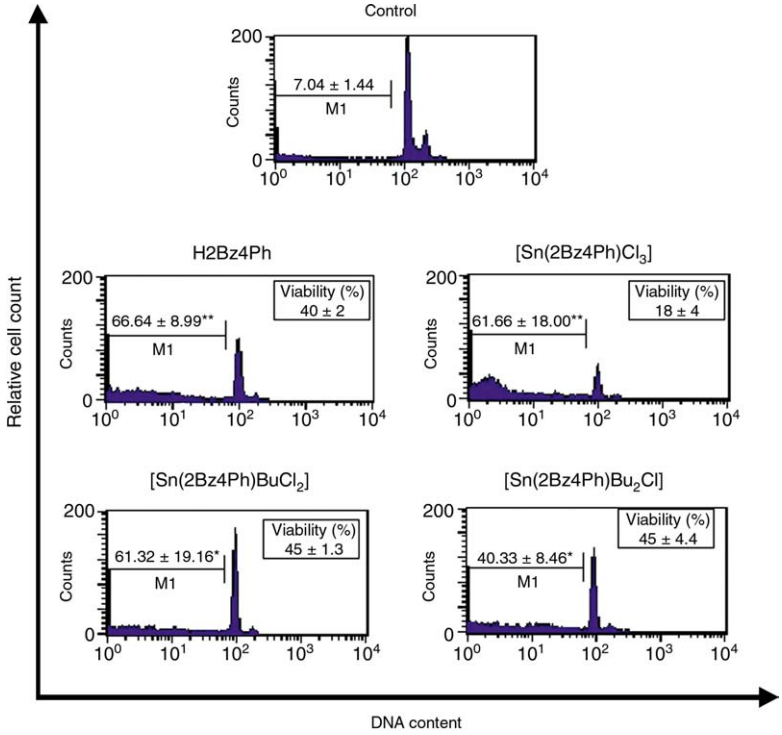

Fig. 7. Representative histograms of the effect of H2Bz4Ph and its Sn(IV) complexes on UACC-62 viability and apoptosis induction. UACC-62 cells were treated for 18 h with different complexes at 10 μg ml^{-1} and viability evaluated using the MTT assay. Apoptosis was determined by PI staining and flow cytometric analysis. The data are presented as the mean ± S.D. for three independent experiments, each in triplicate. Statistically different of control $^{**}P = 0.0001$ and $^{*}P < 0.004$.

[24], we initially investigated the pro-apoptotic potential of these complexes using flow cytometric measurements of DNA fragmentation in the nuclear extracts of UACC-62 cells treated with compounds, as indicative of cell death by apoptosis. The foregoing preliminary studies (Fig. 7) showed that the thiosemicarbazone as well as its three tin(IV) complexes (10 μg ml^{-1}) reduced the cellular viability with enhancement of the percent of apoptotic cells, as assayed by the hypodiploid DNA peak increase in the DNA histogram, suggesting that they kill UACC-62 cells through apoptosis induction. A detailed evaluation of the mechanism by which these complexes induces apoptosis is currently being carried out in our laboratory.

3. Conclusions

The results obtained in the present work indicate that coordination to tin significantly increases the citotoxic activity of H2Bz4Ph. Therefore tin-based antitumoral agents with thiosemicarbazones could constitute a good strategy for the preparation of novel anticancer compounds in the future.

4. Experimental

4.1. Chemistry

H2Bz4Ph was prepared as already described [21]. Complexes **1** and **2** were obtained and characterized previously [21].

4.2. X-ray structure determination

Crystals suitable for X-ray analysis were obtained from an ethanol solution. The intensity data were collected on a CAD4 diffractometer with graphite-monochromated Mo Kα radiation.

The cell dimensions were from least-squares fit of 25 reflections in the range $16° \leq 2\theta \leq 24°$. As check on stability of the diffractometer and of the crystals, three reflections were measured at 60 min intervals during data collection and no significant fluctuation in intensities was observed. The diffracted intensities were corrected for Lorentz and polarization effects and absorptions by the ψ-scan method [25]. The structures were solved by direct methods using Sir-92 [26] and conventional Fourier Synthesis (SHELX-97) [27]. The refinements were performed by full-matrix least-squares on F^2. Anisotropic thermal parameters were applied to the non-H atoms. The H were detected either in a difference Fourier or introduced in calculated positions with thermal parameters 1.2 times that of the attached atom. ORTEP [28] was used for the drawings.

4.3. In vitro cytotoxicity studies (assays with human cancer cell lineages)

The assay with the human cancer cell lines UACC-62 (human melanoma), TK-10 (human renal carcinoma) and MFC-7 (human breast cancer) was run using the protocol established at the National Cancer Institute [29]. In brief, all

adherent cell lines are detached from the culture flasks by addition 1 ml of 0.05% trypsin-EDTA (GIBCO Laboratories, Grand Island, NY). After counting, dilutions are made to give appropriated cell densities for inoculating onto the microtiter plates. Cells are inoculated in a volume of 100 μl per well at densities of 15,000 cells of TK-10 and 10,000 cells of UACC-62 and MCF-7 per well and are preincubated for 24 h at 37 °C to allow stabilization prior to addition of complexes. Subsequently, the different complexes were inoculated incubated for 48 h in an atmosphere of 5% CO_2 and 100% relative humidity. The end point of the procedure was determined by the sulforhodamine B (SRB) method, as described below.

We used the SRB method [29]. Briefly, adherent cell cultures are fixed in situ by adding 50 μl of cold 50% (wt./vol.) tricholoroacetic acid (TCA) and incubated during 60 min at 4 °C. The supernatant is then discarded, and the plates are washed five times with deionized water and dried. One hundred micro liters of SRB solution (0.4% wt./vol. in 1% acetic acid) is added to each well and incubated for 10 min at room temperature. The plates are air-dried and the bound stain is solubilized with Tris buffer and the optical densities are read on an automated spectrophotometric plate reader at 515 nm.

4.4. DNA labeling and flow cytometry analysis to detect apoptosis

In order to detect apoptotic nuclei, UACC-62 cells were treated with different complexes for 18 h. After incubation, the cells were re-suspended in hypotonic solution (50 μg ml^{-1} PI in 0.1% sodium citrate plus 0.1% Triton X-100) [30]. The samples were incubated 4 h at 4 °C, and PI fluorescence of individual nuclei was measured using a FACScalibur flow cytometer (Becton Dickinson Immunocytometry Systems, San Jose, CA). The data were analyzed using the Lysis software (Becton Dickinson). Apoptotic cells were detected on a PI histogram as a hypodiploid peak. The viability of UACC-62 cells was performed in parallel and determined by MTT method [31].

4.5. Statistical analysis

Each experiment with UACC-62 cells was run in triplicate and repeated at least three times in different days. The results were given as the mean ± standard deviation (S.D.). All the data for each experiment were analyzed by Student's *t*-test. Statistical significance was considered when P was ≤ 0.05.

5. Supplementary material

Crystallographic data of the structural analysis for $[Sn(2Bz4Ph)Cl_3]\cdot CH_3CH_2OH$ (**1**), $[Sn(2Bz4Ph)BuCl_2]\cdot H_2O$ (**2**) have been deposited at Cambridge Crystallographic Data Center as supplementary publication number CCDC 253199 (**1**) and 253200 (**2**). Copies of available material can be obtained on application to CCDC, 12 Union Road, Cambridge CB2 1Ez, UK (fax: +44-1223-33-6033 or e-mail: deposit@ccdc.cam.ac.uk).

Acknowledgements

This work was supported by Capes and CNPq of Brazil.

References

[1] H. Beraldo, D. Gambino, Mini Rev. Med. Chem. 4 (2004) 31–39.
[2] D.X. West, A.E. Liberta, S.B. Padhye, R.C. Rajeev, P.B. Sonawane, A.S. Kumbhar, et al., Coord. Chem. Rev. 123 (1993) 49–81.
[3] A. Altun, M. Kumru, A. Dimoglo, J. Mol. Struct. Theochem. 535 (2001) 235–246.
[4] J.G. Cory, A.H. Cory, G. Rappa, A. Lorico, M. Liu, T. Lin, et al., Biochem. Pharmacol. 48 (1994) 335–344.
[5] M.C. Liu, T. Lin, J.G. Cory, A.H. Cory, A.C. Sartorelli, J. Med. Chem. 39 (1996) 2586–2593.
[6] R.A. Finch, M. Liu, S.P. Grill, W.C. Rose, R. Loomis, K.M. Vasquez, et al., Biochem. Pharmacol. 59 (2000) 983–991.
[7] H. Beraldo, L. Tosi, Inorg. Chim. Acta 75 (1983) 249–257.
[8] H. Beraldo, L. Tosi, Inorg. Chim. Acta 125 (1986) 173–182.
[9] A. Abras, H. Beraldo, E. Fantini, R.H. Borges, M.A. da Rocha, L. Tosi, Inorg. Chim. Acta 172 (1990) 113–117.
[10] R.H. Borges, E. Paniago, H. Beraldo, J. Inorg. Biochem. 65 (1997) 267–275.
[11] R.H. Borges, A. Abras, H. Beraldo, J. Braz. Chem. Soc. 8 (1997) 33–38.
[12] D.X. West, I.S. Billeh, J.P. Jasinski, J.M. Jasinski, R.J. Butcher, Transition Met. Chem. 23 (1998) 209–214.
[13] D.X. West, J.S. Ives, J. Krejci, M. Salberg, T.L. Zumbahlen, G. Bain, et al., Polyhedron 14 (1995) 2189–2200.
[14] D. Kuntala, A.K. Guha, Indian J. Chem. Sect. A 29 (1990) 605–607.
[15] S. Sreekanth, M.R.P. Kurup, Polyhedron 22 (2003) 3321–3332.
[16] S. Sreekanth, M.R.P. Kurup, Polyhedron 23 (2004) 1225–1233.
[17] R.F.F. Costa, A. Perez-Rebolledo, T. Matencio, H.D.R. Calado, J.D. Ardisson, M.E. Cortés, et al., J. Coord. Chem. (2005) (accepted).
[18] D. Kovala-Demertzi, P. Tairidou, U. Russo, M. Gielen, Inorg. Chim. Acta 239 (1995) 177–183.
[19] M. Kemmer, M. Gielen, M. Biesemans, D. de Vos, R. Willem, Metal-Based Drugs 5 (1998) 189–196.
[20] M. Gielen, H. Dalil, B. Mahieu, D. de Vos, M. Biesemans, R. Willem, Metal-Based Drugs 5 (1998) 275–277.
[21] A.P. Rebolledo, G.M. de Lima, L.N. Gambi, N.L. Speziali, D.F. Maia, C.B. Pinheiro, et al., Appl. Organomet. Chem. 17 (2003) 945–951.
[22] J. Valdés-Martínez, S. Hernández-Ortega, D.X. West, A.M. Stark, G.A. Bain, J. Chem. Crystallogr. 26 (1996) 861–864.
[23] S. Barbieri, H. Beraldo, C.A. Filgueiras, A. Abras, J.F. Nixon, P. Hitchcock, Inorg. Chim. Acta 206 (1993) 169–172.
[24] S. Carney, Drug Discov. Today 20 (2003) 955–957.
[25] A.C.T. North, D.C. Phillips, F.S. Mathews, Acta Crystallogr. Sect. A 24 (1968) 351–359.
[26] A. Altomare, M.C. Burla, M. Camalli, G. Cascarano, C. Giacovazzo, A. Gagliardi, et al., J. Appl. Crystallogr. 27 (1994) 435–436.
[27] G.M. Sheldrick, SHELX-97. Program for the Refinement of Crystal Structures, University of Göttingen, Germany, 1997.
[28] C.K. Johnson, ORTEP 11, Report ORNL-5138, Oak Ridge National Laboratory, TN, 1976.
[29] A. Monks, D. Scudiero, P. Skehan, R. Shoemaker, K. Paull, D. Vistica, et al., J. Natl. Cancer Inst. 83 (1991) 757–766.
[30] I. Nicoletti, G. Migliorati, M.C. Pagliacci, F. Grignani, C. Riccardi, J. Immunol. Meth. 139 (1991) 271–279.
[31] J. Jiang, Q. Xu, J. Ethnopharmacol. 85 (2003) 53–59.